Flagging the Topographic Impact on the SMOS Signal

Arnaud Mialon, Laurent Coret, Yann Kerr, Jean Pierre Wigneron

Flagging the topographic impact on the SMOS signal

Arnaud Mialon, Laurent Coret, Yann H. Kerr, *Member 88, Senior Member 01, IEEE,* François
Sécherre, Jean-Pierre Wigneron, *Senior Member 03, IEEE*

Abstract

Soil moisture retrieval models from Soil Moisture and Ocean Salinity (SMOS) mission, an L-band
microwave interferometer, are based on multi-angular measurements and make use of the emissivity angular
signature. Mountainous areas modify local incidence angles, implying significant impacts on brightness
temperatures and, consequently, on soil moisture retrievals. The purpose of this study is to establish a
criterion to quantify the relevance of topographic impacts at the SMOS scale ($\sim$40 km). The goal is thus
to define a method to flag the pixels according to the relative impact of topography on the brightness
temperature. The proposed method uses the variogram of digital elevation model (DEM) images.

As a result, a map of pixels to be flagged is produced to ensure no soil moisture retrievals are carried
out on pixels which are affected by a strong topographic effects. As validation, a model was also used
to simulate differences between brightness temperature variations between mountainous areas and flat
surfaces.

Index Terms

SMOS, Topography impacts, Passive Microwave, L-band.

I. Introduction

The SMOS mission, part of ESA's (European Space Agency) Earth Explorer Opportunity program,
is a 1.4 GHz (L-band) multi-angular interferometer [1]. It is scheduled for launch in 2008. One of
the main scientific objectives is to retrieve soil moisture with an accuracy of 4% [1]. Soil moisture
retrieval schemes from SMOS data are based on multi-angular measurements of a scene, using the
incidence angle dependency of the emissivity [2]. Consequently, topography, characterized by various
facets, varying slopes, shadowing and adjacency effects, can significantly alter the relationship between
reflectivity and incidence angle of a surface and the optical thickness of the canopy [3]-[4] and affect
surface emission. Moreover, the distribution of vegetation with altitude and the distribution of water are
linked to topographic features (altitude and slopes). This leads to impacts on the measured brightness
temperatures up to several kelvin depending on the incidence angle [3] - [5] that may imply uncertainties

A.Mialon, L. Coret and Y.Kerr are with the Centre d'Etudes Spatiales de la Biosphère (CESBIO), Toulouse, France.

J.P. Wigneron is with the Institut National de Recherche Agronomique (INRA), Bordeaux, France.

on soil moisture higher than the 4% required. Few attempts have been dedicated to estimate topography impacts on L-band brightness temperatures. Because of the complexity of simulation, retrieval models are designed for flat surfaces. They do not, *per se*, allow to take these perturbations into account.

Therefore, within the framework of soil moisture retrieval, an important issue is to assess, through a quantitative estimator, to which of three classes a SMOS pixel (node) is to be assigned. These three classes are : flat surface (i.e. soil moisture retrieval possible), moderate topography (flagged pixels and soil moisture retrieval attempted) and strong topography (precludes any sensible soil moisture retrieval at the SMOS scale). According to [5], this criterion should rather rely on the slope distribution itself and not on a surrogate variable related to slope distribution such as altitude. Considering this, we proposed here a simple method applicable at a global scale and based on a Digital Elevation Model (DEM). Results presented in this paper are used to generate a map of flagged pixels to be used in the SMOS soil moisture level 2 retrieval.

II. RATIONALE

As no detailed measurement data are available on the issue of topography effect on L-band brightness temperatures, previous studies [3],[4], have attempted to characterize topographic impacts on passive microwave measurements with models. A first approach was developed by [4] to simulate the effect due to tilted surfaces from a flat surface. This allowed to quantify variations of the incidence angle and the shadowing effect (radiation of surrounding elevated surface). This model was then generalised by [5] using a geometrical approach accounting for shadowing and adjacency effects. Based on a radiative transfer model [6] and surface emissivity from the L-MEB (L-band Microwave Emission of the Biosphere) model [7], the upwelling emission can be computed in any direction. The approach consists in considering first the emission from a flat surface. Then, the same surface properties are projected on tilted surfaces. Differences between the two simulated radiations (called ΔTb) are linked to topography. Applying this model (hereafter refered as the ΔTb model) is not feasible at a global scale because the process is too ressource demanding (L-Meb and its many inputs, geometrical approach including angle computation and shadow effects...) in the L2 soil moisture scheme. Moreover, soil moisture and vegetation may vary with altitude and slope which is not taken into account with this model, though it is important [9]. However, we use this ΔTb model over the Pyrenees (West-East orientation), the Alps (more random slope distribution) and over the Andes (North-South orientation) to assess the merit of the new method proposed in this study.

Kerr et al.'s study [5] also reported two important considerations for our purpose. First, the criterion we want to define must rely on slope distribution and not on the altitude. Secondly, slope distribution can be effectively categorized into three different terrain types (Fig. 1). Almost flat surface - plains (Fig. 1 a) - can be characterized by a mean slope less than 2° and a low variance. High topography - rugged areas (Fig. 1 c)- have high mean slopes, with a low variance. And finally, an intermediate case is related to
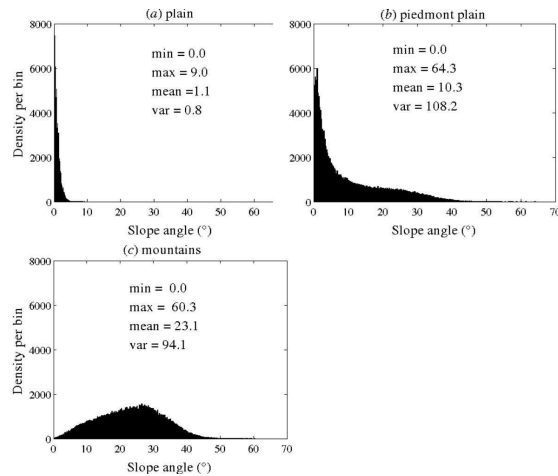
Fig. 1.   Histograms of slope distribution for 3 topographic landscapes : a) plain ; b) piedmont plain (i.e.,areas lying at the foot of mountain range) ; c) mountain (i.e. rugged terrain).
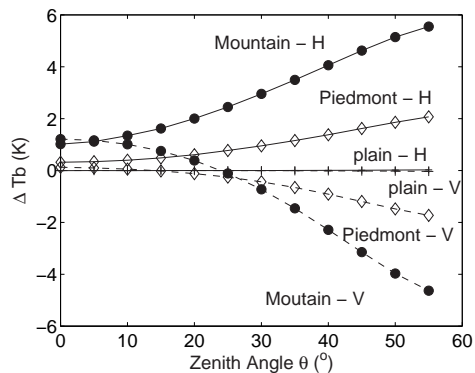

Fig. 2.   Angular representation of Δ Tb for both polarizations (H, continued lines and V dashed lines) for different terrains : plain (+) ; piedmont plain (◇) ; mountain (●).

areas lying at the foot of mountain range, called piedmont plain. It is a mixture of plain and moutainous areas (Fig. 1 b), associated with a mean slope close to 10° and a high variance due to larger range of slopes.

Using the ΔTb model for these three classes shows the influence of topography on the brightness temperature (Fig. 2). ΔTb depends on the polarization, increasing with zenith angle at H polarization and decreasing at V polarization. For instance, topography can cause ΔTb up to 5K at 55° (limit angle for SMOS studies), illustrating the significant effect of mountainous terrains and hence the importance of locating these areas for SMOS retrievals.

The method proposed here is based on the variogram of a DEM image. The DEM is provided by the Shuttle Radar Topography Mission (SRTM) [10], a joint project between the National Aeronautics and Space Administration (NASA) and the National Geospatial-Intelligence Agency (NGA). Flown aboard the NASA Space Shuttle Endeavour (February 11-22, 2000), the SRTM has collected data over 80 % of
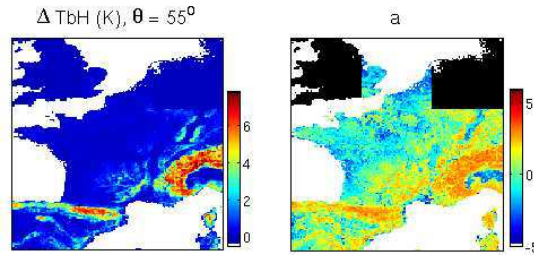
Fig. 3. At left, the spatial variation of the impact on the brightness temperature over Western Europe as predicted by the ΔTb model. At right, the spatial variation of the parameter a from (2) over Western Europe.

the Earth's land surface, between 60° N. and 56° S. of latitude. The dual radar antennas (Spaceborne Imaging Radar-C, SIR-C, and X-band Synthetic Aperture Radar -X-SAR-) provide data at a 3-arc-second resolution (approximately 90 m at the equator).

III. METHOD

A semi-variogram is often used to analyse landscape distribution as forests, urban or agricultural areas. This statistical tool relies on spatial pattern analysis of the landscape [11] and provides an easy method for characterizing land surface topography [12]. The semi-variogram γ(h) of an image is the average square difference of values separated by a number of h pixels [13]:

$$\gamma(h) = \frac{1}{2 \times N(h)} . \sum_{i=1}^{N(h)} [s(h+p_i) - s(p_i)]^2 \qquad (1)$$

where s(p) is the value of the pixel p, and N(h) the number of pairs for lag h. For most geostatistical analysis, mathematical models are used to fit semi-variogram shape [14].

A. Modelling the Semi-Variogram behaviour

The first step of the approach is to model the shape of the semi-variogram [15]. Several analytical models were tested (i.e. affine, fractal and power, exponential) and the most efficient approach was found to be a log-polynomial model (2), based on fractal parameterisation [14] of the landscape, defined as :

$$\gamma(h) = exp(a.(ln(h))^2).h^b.e^c \qquad (2)$$

Between the three parameters of the log-polynomial model (i.e. a, b and c in (2)), a is the most correlated with the topography. This is illustrated in Fig. 3 which shows the spatial distribution of a over Western Europe (right Fig. 3) and the spatial distribution of ΔTb (left Fig. 3 ; horizontal polarization, θ = 55°).

Fig. 4 shows the ΔTb variations for a 55° zenith angle (ΔTb <0 for V polarization and ΔTb>0 for H) as a function of a (from log-polynomial law, (2)) for the same area as depicted in Fig. 3. As suggested
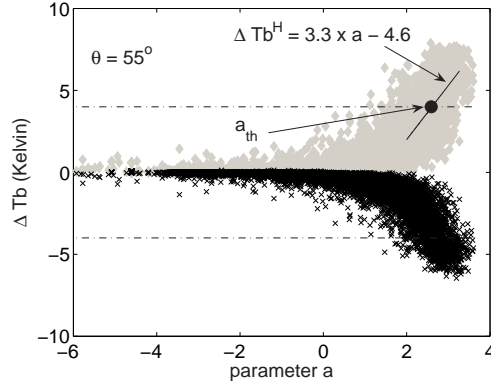
Fig. 4. Δ Tb variation with a-parameter at H polarization (gray $\diamond$) and V polarization (black $\times$). A linear fit is shown (black line) for pixels with $a > 2$ and defined by ΔTb^H = 3.3x a - 4.6. a_{th} is the intersection between the linear fit and ΔTb^H = 4K.

by the behaviour of the data Fig.4, an empirical relationship exists between the two parameters. Using the form of an exponential law, the empirical relationship (not shown in Fig.4) is:

$$\Delta Tb^i(\theta, a) = C_1^i(\theta).exp(C_2^i(\theta).a) \qquad (3)$$

with i the polarization, C_1 and C_2 being empirical constants.

B. Definition of a threshold

Using this function (3), a threshold for the parameter a - hereafter a_{th} - is derived and equal to 2.70 (not shown). This threshold corresponds to $|\Delta Tb|$ = 4K, which is the instrument precision specification [16]. Indeed, it is difficult and not straightforward to estimate variations of Tb from the 4% uncertainties required for the soil moisture retrieval. So we propose here to use the instrument precision specification to deduce a_{th}. Only pixels with a lower than a_{th} are retained, as a higher than a_{th} should indicate high topographic impacts.

IV. RESULTS AND DISCUSSION

Table I (middle column) presents the results of the comparison between pixels having a ΔTb higher than 4 K and pixels having a a higher than a_{th}. 54.6 % of non-wanted pixels (i.e. ΔTb >4) have a a higher than a_{th}. That means only 54.6% of the non-wanted pixels are eliminated when a_{th} threshold is used. This is not acceptable and consequently, another fit function is needed to derive a more appropriate value of a_{th}.

According to Fig.4, only pixels with an a greater than 2 have the potential to result in a $|\Delta$Tb$| > 4$ K. A linear relationship (continued line Fig.4) is applied to fit the ΔTb variations with a for this data range:

TABLE I

NUMBERS AND PERCENTAGE OF PIXELS INFLUENCED BY TOPOGRAPHY (I.E. WITH ΔTB >4K) WHICH ARE ELIMINATED AND
PERCENTAGE OF PIXELS NOT INFLUENCED BY TOPOGRAPHY (I.E. WITH ΔTB ≤4K) WHICH ARE KEPT BY THE USE OF TWO ATH
THRESHOLDS : FROM AN EXPONENTIAL FIT (MIDDLE COLUMN) AND FROM A LINEAR FIT (RIGHT COLUMN). FOR $\Theta = 55^o$ AND
H POLARIZATION, OVER WESTERN EUROPE AND THE ANDES

	ath = 2.70 (exponential fit)	ath = 2.59 (linear fit)
Western Europe		
Pixels influenced by topography, i.e. ΔTb>4K	978	978
% eliminated, i.e. a>ath	54.6%	66%
Pixels not influenced by topography, i.e.ΔTb≤4K	21412	21412
% kept, i.e. a≤ath	99.5%	99.2%
The Andes		
Pixels influenced by topography, i.e. ΔTb>4K	1421	1421
% eliminated, i.e. a>ath	61.9%	74.7%
Pixels not influenced by topography, i.e. ΔTb≤4K	13579	13579
% kept, i.e. a≤ath	97.3%	96.1%

$$\Delta Tb = 3.3 \times a - 4.6 \qquad (4)$$

The same $|\Delta Tb| = 4$ criterion allows to define a new a_{th} (dot pointed out by arrow labeled a_{th}). For $\theta = 55^o$, it is equal to 2.59 at H polarization (dot in Fig. 4) and 2.93 at V polarization. Applying this new threshold, 66% of non-wanted pixels (i.e., having a $\Delta Tb > 4$) are eliminated (Table I, right column).

This result is satisfying enough for our purpose (Fig 5) as much as a confidence interval (see further) is defined around a_{th}. The upper part of Fig. 5 shows results over Western Europe (tile centred over France). Red pixels correspond to areas associated with a higher than a_{th} (here $a_{th} = 2.59$ for H polarization at 55°), and yellow lines outline areas with significant topographic impacts from ΔTb model. The two areas are in good agreement.

As this method should be applicable at a global scale, another area is selected to test the consistency of the resultant map. It is applied over the Andes while the ΔTb model [5] was used as well for comparison. Results (bottom Fig. 5) are better than over Western Europe, with 74.7% (Table I) of non-wanted pixels (i.e. with $|\Delta Tb| > 4K$, from ΔTb model, [5]), eliminated. This can be explained by a different geomorphology between the Andes and the Alps, the latter being qualified as subdued [17] in comparison with the former. It means that the Andes are a more rugged area. This results in the a variation with ΔTb being slightly different than for the Alps (Fig. 4). The linear regression derived from the Andes dataset would have lead to a stronger slope (5) than that from the Alps (4).
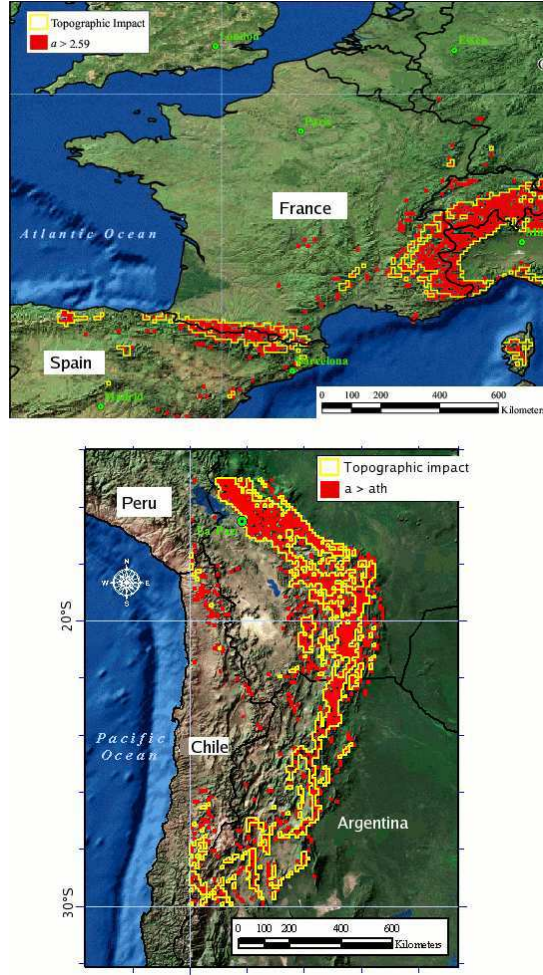
Fig. 5. Comparison between topographic impacts on Tb (yellow boundary) for $\theta = 55^o$ - H polarization, and pixels with a > ath=2.59 (red area), over western Europe (top) and over the Andes (bottom).

$$\Delta Tb = 2.7 \times a - 3.4 \qquad (5)$$

The consequence is that, over the Andes, more pixels with a ΔTb higher than 4K have a a-value higher than a_{th}.

These results are considered satisfying enough for its use in the SMOS level 2 soil moisture retrieval and for a global scale application. Indeed, it is of purpose during the calibration/validation phase of the SMOS mission to tune this method and get to a better accuracy with the availability of real data.

A. Confidence interval

However, uncertainties in ΔTb model have to be considered and are estimated to +/-1.5K. This means that the criterion ΔTb = 4K, used to assess a_{th}, has to be associated with uncertainties equal to +/-1.5K. This implies a confidence interval on a_{th}, which, at 55° and H polarization, corresponds to the range :

[2.17 - 3.04].

B. Classifying the pixels

Computing a for each pixel allows us to distinguish 3 cases. First, if a is lower than the minimum of the confidence interval (i.e., $a < 2.17$ at 55° and H pol.), the surface of the pixel is considered flat and topography would have no detectable influence on SMOS observed brightness temperatures. This represents almost 87.6% of global surface land pixels. Second, if a is in the confidence interval the topography is moderate and there is a slightly detectable influence on the brightness temperature. This is the case for 5.7% of global land surface pixels. Finally, 6.7% of land pixels are characterized by a higher than the maximum value of the confidence interval (i.e., $a > 3.04$ at 55° and H pol.). In this case, topography has an influence on brighness temperature higher than the noise and is thus clearly observable.

A problem with the use of the SRTM DEM is observed at the coasts and borders of water areas which exhibit an important value of a_{th}. There is a a noticeable difference between the elevation of coastal pixels and the elevation of adjacent water pixels, which implies a sharp slope between those pixels and so a high value of a, misclassifying the pixel. However, this issue is easily accounted for with a land sea mask.

V. CONCLUSION

The SMOS mission will provide multi-angular data at L-band (1.4 GHz). One of the main objectives is to measure soil moisture on continental surfaces. However, microwave satellite measurements can be strongly affected by topography. Indeed, since topography modifies incidence angle, significant effects on soil moisture retrieval schemes, based on multi-angular measurements, are induced. Topographical features can cause brightness temperature variations up to 5K [18]. Depending on surface properties (soil moisture and vegetation optical thickness), this may lead to soil moisture retrieval errors higher than the required accuarcy (4% [1]). Current soil moisture retrieval models do not take topography into account. In this paper, a first attempt is presented to identify SMOS pixels affected by topography at a global scale. This simple method is based on semi-variograms of a DEM map. Moreover, it is easier to implement in the soil moisture retrieval scheme than the ΔTb model. A log-polynomial function is first used to fit the semi-variogram behaviour. Then, a relationship is established between one parameter (referred to as a) of this function and brightness temperature variations due to topography (according to ΔTb model [5]). The instrument uncertainties ($|\Delta$Tb$| = 4$K) allows to establish an arbitrary threshold value to be adjusted during the commissionning phase, depending on the incidence angle and polarization. Uncertainties on ΔTb model lead to consider a confidence interval for a_{th}.

The method developed over the Alps and Pyrenees in Europe has been applied over the Andes (characterized by a different orientation) and offers promising results. A global map of flagged pixels is then deduced and can be used in the level2 soil moisture retrieval schemes [8]. SMOS nodes with a

lower than the minimum value of the confident interval are considered not influenced by topography and soil moisture is attempted ; for nodes presenting a a-value between the minimum value of the confidence interval and a_{th}, topography is considered having a moderate impact, so soil moisture is attempted with bigger error bars ; finally, nodes having a a-value higher than a_{th}, are masked and no soil moisture retrieval is attempted.

As acceptable as the method may be in the framework of SMOS L2, improvements are possible to enhance accuracies. It is planned to tune the threshold during the calibration/validation phase of the SMOS mission when data will be available. Investigations on the fit function between a and ΔTb can improve both a and the confidence interval. Validation studies should also be carried out with the use of other satellite data (Polarization Index of SMMR or AMSR). And finally, further efforts will focus on assessing the threshold a_{th} considering the relationship between a and the soil moisture variations due to topography by using retrieval models.

REFERENCES

[1] Y. Kerr, P. Waldteufel, J. Wigneron, J. Font, and M. Berger, " Soil moisture retrieval from space : the Soil Moisture ant Ocean Salinity (SMOS) mission ," *IEEE T. Geosci. Remote*, vol. 39(8), pp. 1729–1735, 2001.

[2] J.-P. Wigneron, P. Waldteufel, A. Chanzy, J. Calvet, and K. Y., "Two-D microwave interferometer retrieval capabilities of over land surfaces (smos mission)," *Rem. Sens. Environ.*, vol. 73(3), pp. 270–282, 2000.

[3] C. Mätzler, P. Rosenkranz, A. Battaglia, and J.-P. Wigneron, *Thermal Microwave Radiation - Applications for Remote Sensing*.   IET Electromagnetic Waves Series 52, London, UK, 2006.

[4] C. Mätzler and A. Standley, "Technical note - relief effects for passive microwave remote sensing," *Int. J. Remote Sens.*, vol. 21(12), pp. 2403–2412, 2000.

[5] Y. Kerr, F. Secherre, J. Lastenet, and J.-P. Wigneron, "SMOS : analysis of perturbing effects over land surfaces," *Geoscience and Remote Sensing Symposium, 21-25 July 2003. IGARSS '03. Proceedings. 2003 IEEE International*, vol. 2, pp. 908– 910, 2003.

[6] Y. Kerr and E. Njoku, "A semi empirical model for interpreting microwave emission from semiarid land surfaces as seen from space," *IEEE T. Geosci. Remote*, vol. 28, pp. 384–393, 1990.

[7] J.-P. Wigneron, Y. Kerr, P. Waldteufel, K. Saleh, M.-J. Escorihuela, P. Richaume, P. Ferrazzoli, P. de Rosnay, R. Gurney, J.-C. Calvet, J. Grant, M. Guglielmetti, B. Hornbuckle, C. Mätzler, T. Pellarin, and M. Schwank, "L-band Microwave Emission of the Biosphere (L-MEB) Model : Description and calibration against experimental data sets over crop fields," *Rem. Sens. Environ.*, vol. 107, pp. 639–655, 2007.

[8] Y. Kerr, P. Waldteufel, P. Richaume, J. Wigneron, P. Ferrazzoli, and R. Gurney, "SMOS level 2 processor for soil moisture - Algorithm Theoretical Based Document (ATBD) ," CBSA, Tech. Rep. SO-TN-ESL-SM-GS-001, Issue 2, 2006, 212 p., http://www.cesbio.ups-tlse.fr/fr/indexsmos.html.

[9] J. Pellenq, J. Kalma, G. Boulet, S. Saulnier, G.-M.and Wooldridge, K. Y., and A. Chehbouni, "A disaggregation scheme for soil moisture based on topography and soil depth," *J. Hydrolo.*, vol. 276(1-4), pp. 112–127, 2003.

[10] A. Jarvis, H. Reuter, A. Nelson, and E. Guevara, "Hole-Filled seamless SRTM data V3," 2006, International Centre for Tropical Agriculture (CIAT), available from CGIAR-CSI SRTM 90m database http.//srtm.csi.cgiar.org.

[11] N. Tate, "Estimating the fractal dimension of the synthetic topographic surfaces," *Comput. Geosci.*, vol. 24-4, pp. 325–334, 1998.

[12] C. McClean and E. I.S., "Apparent fractal dimensions from continental scale Digital Elevation Models using Variogram methods," *Trans. on GIS*, vol. 4(4), pp. 361–378, 2000.

[13] G. Mathéron, *The theory of regionalized variables and its application*.   Les cahiers du Centre de Morphologie Mathématique de Fontainebleau, 1971, vol. Fasc. 5, ENSMP, Paris, 212 p.

[14] R. Webster and M. Oliver, *Statistical methods in soil and land resource survey*.   Oxford University

Press, 1990.

[15] L. Coret, Y. Kerr, and P. Richaume, "Flagging the topographic impact on the SMOS signal," 2006, CESBIO SMOS Technical note: SO-TN-CBSA-GS-0012, Issue: 1.b, 27 p., http://www.cesbio. ups-tlse.fr/fr/indexsmos.html.

[16] Y. Kerr, J. Font, P. Waldteufel, A. Camps, J. Bara, I. Corbella, F. Torres, N. Duffo, M. Vall.llossera, and G. Caudal, "Next Generation radiometers: SMOS a dual pol L-band 2D aperture synthesis radiometer," *P.Pampaloni and S. Paloscia, Eds., Utrecht, The Netherlands*, pp. 447–483, 2000.

[17] J. Kley and G. H. Eisbacher, "How Alpine or Himalayan are the Central Andes?" *International Journal of Earth Sciences*, vol. 88, pp. 175–189, 1999.

[18] Y. Kerr, F. Sécherre, R. Gathier, and J.-P. Wigneron, *Analysis of topography effect*, 2004, complement to ESA, ITT-3552 (CNN).